



# COVID-19 aerodynamic evaluation of social distancing in indoor environments, a numerical study

A. R. Sarhan<sup>1</sup> · P. Naser<sup>2</sup> · J. Naser<sup>1</sup>

Received: 25 February 2021 / Accepted: 17 October 2021 / Published online: 25 October 2021  
© Springer Nature Switzerland AG 2021

## Abstract

**Purpose** Many countries worldwide have taken early measures to combat the spread of coronavirus SARS-CoV-2 by implementing social distancing measures. The main aim of the present work is to examine the feasibility of social distancing (i.e. 1.5 m) in closed spaces taking into account the possibility for airborne transmission of SARS-CoV-2.

**Methods** A 3D numerical model of human respiration activities, such as breathing and speaking within indoor environments has been simulated with CFD software AVL FIRE R2020. The Eulerian-Eulerian flow model coupled with k- $\epsilon$  approach were employed. With regard to breathing mode, the infected individual is modelled to be breathing 10 times per minute with a pulmonary rate of 6 L/min with a sinusoidal cycle. The present investigation considered air and droplets/particles as separate phases.

**Results** The predicted results suggested that the social distancing (i.e. 1.5 m) is not adequate to reduce the risk of contracting diseases like COVID-19, especially when staying for a longer period in an indoor environment. The person directly facing the infected person inhaled more than 1000 aerosol droplets within 30 min. The results also showed approximately 65% decrease in the number of inhaled droplets the room is well ventilated.

**Conclusions** Within an indoor environment, 1.5 m distance will not be enough to protect the healthy individuals from the droplets coming from an infected person. Also, the situation may become worse with the change of the air ventilation system.

**Keywords** COVID-19 · Social distancing · Airborne transmission · Droplets · Indoor environments · CFD

## Introduction

Coronaviruses are a large family of viruses that usually cause mild to moderate upper-respiratory tract illnesses, like the common cold. However, three new coronaviruses have emerged from animal reservoirs over the past two decades to cause serious and widespread illness and death [1]. Coronaviruses consist of a core of genetic material surrounding by lipped enclosed within an envelope of protein spikes, which give them the appearance of a crown (or, in Latin, corona). Coronavirus SARS-CoV-2 is a clinical disease caused by a new form of coronavirus represents a major worldwide

health risk [1, 2]. It was first reported in December 2019 in Wuhan City in China [3]. SARS-CoV-2 never travels alone, but always in an aqueous environment [4–6]. Most of the early research on this topic stated, there is no evidence on the possibility for airborne transmission SARS-CoV-2 [3, 7–9]. It was assumed that the transmission of the virus between humans occurs only through direct contact with an infected individual [3]. However, recent evidence suggests that the transmission of COVID-19 may occur through droplets transmission, contact transmission [1, 2, 10] or aerosol transmission [11–13].

In the middle of 2020, the possibility for airborne transmission of the virus was discussed by several studies [3–5, 7–9]. These studies provided an insightful argument about the possibility of transmission by mixing droplets containing the virus with the air and then being inhaled by a healthy individual [12, 13]. Group of researchers evaluated the stability of SARS-CoV-2 and SARS-CoV-1 in aerosols and on various surfaces and estimated their decay rates using a Bayesian regression model [9]. Their results

✉ A. R. Sarhan  
asarhan@swin.edu.au

<sup>1</sup> Department of Mechanical and Product Design Engineering,  
Swinburne University of Technology, Hawthorn,  
Victoria 3122, Australia

<sup>2</sup> Johns Hopkins Bloomberg School of Public Health,  
Baltimore, MD 21205, USA

showed that SARS-CoV-2 can remain airborne in a room for several hours. In an investigation into the transmission of SARS-CoV-2 in a restaurant in China, Lu, et al. [3] demonstrated that airborne transmission by the ventilation system was responsible for these infections. Their findings can only be explained if aerosol particles are small enough to be transported by the air over a certain distance. Liu, et al. [14] conducted an aerodynamic analysis of room air at different Wuhan hospitals. They were able to detect significant amounts of SARS-CoV-2 viruses in the size range of 0.25–0.5  $\mu\text{m}$  within one protective apparel removing room. They also were able to trace particles between few nanometres and 10  $\mu\text{m}$ . In their thorough investigation of SARS-CoV-2, Morawska and Cao [13] concluded that the SARS-CoV-2 epidemic is also influenced, at least to a large extent, by the transmission of exhaled aerosolized viruses, and this must be taken into account to contain the pandemic. Scheuch [4]’s comprehensive review concluded that there is a strong scientific rationale and evidence that viruses are very efficiently spread through aerosols by the patient’s breathing only. It is not necessary for the patient to cough or sneeze. Research showed that SARS-CoV-2 can be stable up to 24 h on cardboard, 2–3 days on plastic and stainless steel, and up to 3 h in an aerosol which includes fog, dust and smoke. Therefore, it is possible to get infected by touching a contaminated surface or through the air. This is what made COVID-19 highly contagious, as the number of cases reached more than 32 million as of September 2020 [1].

Human respiration activities, such as breathing, speaking, coughing, sneezing or laughing release thousands of droplets and aerosols into the air [4]. The number, velocity and size distributions of droplets vary depending on the type of activity. The characteristics of droplets (i.e. number and size) have important implications for transmission. The larger droplets, which carry more virus particles, settle more quickly due to gravity. The smaller droplets, carrying fewer particles, may remain suspended in the air for hours. Therefore this topic has been attracting a lot of attention and numerous studies have attempted to determine the number and the size of these droplets during breathing and speaking

[15–22]. These studies were done on a group of a healthy individuals [15–18, 20, 21], and a group of subjects who were infected with influenza [19]. The results of these studies revealed that normal breathing can generate an order of ( $10^3$ ) or more droplets per litre, with average size varies from 0.3 to 5  $\mu\text{m}$ . On the other hand, data showed that speaking may release 10 times more droplets into air, with average size varies from 5 to 75  $\mu\text{m}$  [15, 16]. Although some of these studies [17, 21] found that the majority of particles during expiratory activities were less than 1  $\mu\text{m}$  in diameter. Table 1 shows the size distribution of droplets found in breathing and speaking reported in previous studies.

Many countries worldwide have taken early measures to combat the spread of the virus by implementing social distancing measures. Social distancing means maintaining a distance or space between people to stop or slow down the spread of infectious diseases. France, Denmark and China recommend social distancing of one metre; Australia, Italy and Germany recommend 1.5 m, and the US recommends 1.8 m [1, 2, 10, 25]. This distance was chosen based on assumption that most of the respiratory droplets fall due to gravity and reach the floor and/or evaporate before having travelled a distance of 1.5 m [10]. To the best of the authors’ knowledge, airborne transmission of the virus was ignored by the majority of CFD studies that address the effect of social distancing [26]. Therefore, the main objective of this study is to examine the feasibility of social distancing (i.e. 1.5 m) in indoor environments taking into account the possibility for airborne transmission of SARS-CoV-2.

## Numerical procedures

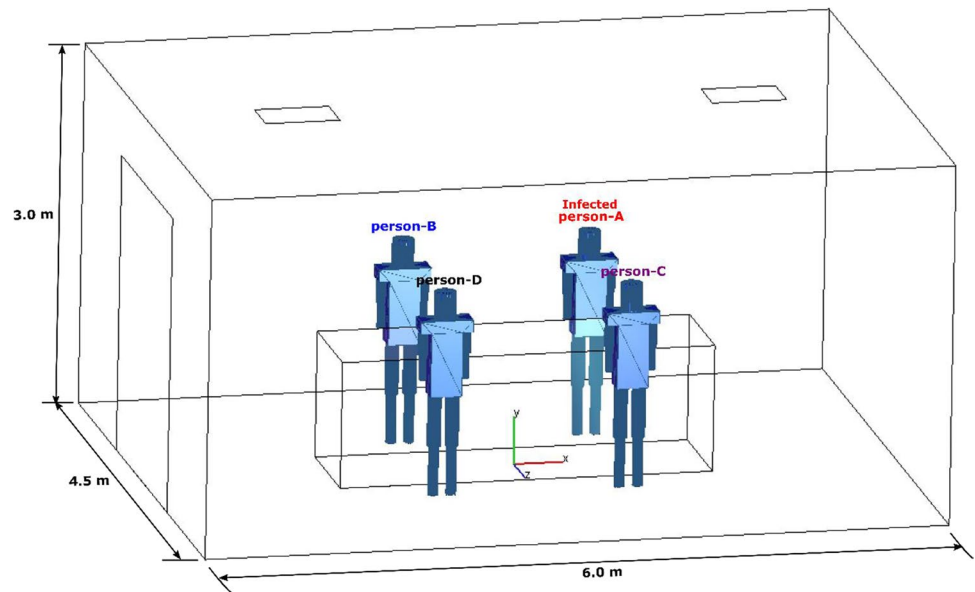
### Model description and grid sensitivity analysis

In the present study, human respiration activities, such as breathing and speaking within indoor environments has been simulated with CFD. CFD software AVL FIRE R2020 was used in the present study. Figure 1 illustrates the geometry used in the present model. The room has dimensions of

**Table 1** Previous literature on the droplet size distribution of respiratory activities

Reference	Country	Method	Respiratory activity	Droplet size
[15]	Scotland	stain-marks on slides	loud speech	5 - 500 $\mu\text{m}$
[17]	USA	optical particle counter & analytical electron microscope	breath & speech	> 1 $\mu\text{m}$
[18]	USA	optical particle counter	breath	0.15 – 0.19 $\mu\text{m}$
[19]	USA	optical particle counter	breath	> 1 $\mu\text{m}$
[20]	China	imaging technique	speech	$\geq$ 16 $\mu\text{m}$
[21]	Australia	expiratory droplet investigation system	breath & speech	> 1 $\mu\text{m}$
[23]	China	optical particle counter	speech	50 – 100 $\mu\text{m}$
[24]	USA	aerodynamic particle sizer	loud speech	0.5 – 20 $\mu\text{m}$

**Fig. 1** Computational domain showing the location of the infected person in an enclosed environment



4.5 m-width  $\times$  6 m-depth  $\times$  3 m-height. Two cases were investigated; case-1, the room was naturally ventilated with air incoming through the door. While, in case-2, the door was closed, and the room was ventilated with a constant airflow of  $0.045 \text{ m}^3 \cdot \text{sec}^{-1}$  through two holes, located on the ceiling of the room. This room is occupied with four individuals, the height of each individual is 1.75 m. The distance between the individuals is assumed to be 1.5 m. To examine the feasibility of social distancing (i.e. 1.5 m) in closed spaces taking into account the possibility for airborne transmission of SARS-CoV-2 through breathing and speaking, one individual was assumed to be infected with COVID-19. With regard to breathing mode, the infected individual is modelled to be breathing 10 times per minute with a pulmonary rate of 6 L/min with a sinusoidal cycle (3-sec inhalation + 3-sec exhalation) [6, 8, 27]. The present investigation considered air and droplets/particles as separate phases. Little is known about the aerosols produced by COVID-19 infected subject. However, the size of SARS-CoV-2 (i.e. 60 nm – 160 nm) is very similar to the size of influenza viruses (80 nm – 100 nm) [1, 4, 5, 10, 13, 28]. Researchers reported that the concentration of aerosol particles in human exhaled breath  $\sim 10,000$  particles per litre [19, 28]. Therefore, one exhaled breath, which is between 0.3 and 0.75 L [29] could contain an order of  $10^3$  droplets ( $\geq 1 \mu\text{m}$ ) [30]. The size of these aerosol particles is small enough to remain suspended in air and present a risk for airborne transmission.

Based on the presence of each of the droplet concentrations, different regions can be identified in the computational domain. The average size of the droplets was assumed to be  $1.0 \mu\text{m}$  [11, 16, 24, 31]. The transport equations for all phases throughout the whole domain are solved to cater for the transient dynamic situation in the domain. To obtain an

acceptable accuracy with acceptable computational time, various grid independency tests were conducted with different mesh resolutions. Two different grids of the model were generated by using the FAME Hexa meshing technique with a control volume of 1,125,000 and 1,726,000 cells where each grid has a similar meshing scheme. To evaluate the impact of the grid on the results, simulations were carried out on both grids. It has been verified that the percentage of change in the solution in both cases is small. Also, it was found that there were no significant differences in the results. Therefore, the mesh consisting of 1,125,000 numerical meshes was chosen for further simulations.

### Description of the mathematical model

The AVL CFD solver which is based on the Finite Volume Method (FVM) is used in the present work to solve the governing equations of the multi-phase flow within the computational domain [32]. The numerical algorithm of this approach consists the following steps; integrating the governing equations over the control volumes of the computational domain, converting the results of integration step into a system of algebraic equations, and finally using an iterative method to solve the algebraic equations. The first-order Euler scheme was employed in the present model to discretise the flow equations. This scheme is reasonable compared to the second-order scheme which is computationally expensive (i.e. requires more simulation time and memory) [33]. The turbulence models are implemented for accurate calculations of turbulent flows. The SIMPLE method is employed to determine the pressure [34]. In this method, the discretised form of the momentum equations is solved using the guessed value of the

pressure field to yield velocity components. The difference between the correct pressure and the guessed pressure represents the correction pressure. The correction pressure is then employed to update the velocity and pressure fields in the momentum equation, respectively. Therefore, the velocity components that obtained from the momentum equations satisfy the continuity equation. The generalized zero levels fill-in orthomin solver (GSTB) is employed in this study as a linear solver for the solution of the main equations (i.e. Momentum, Continuity, Turbulence and scalar). In this study mass source residual (error in continuity) was used to control the convergence of the solution and the tolerance limit was set to  $10^{-4}$ . In this simulation, the equation for continuity, momentum and transport equation for  $k$  and  $\epsilon$  were solved for turbulence parameter. The simulation time was 3600 s and the time step were 0.01 s for all simulation cases in this study.

In the present model, the gas (continuous phase) and droplets/particles (dispersed phases) are each characterized by a set of continuum equations describing the conservation of mass and momentum within a fixed control volume. As mentioned earlier, air and droplets/particles treated as two different independent phases and their movement is taken in Eulerian reference frame. The interactions between phases are accounted through various interfacial forces. In the computational domain, the different phases interacted and interpenetrated with each other. The concept of phase volume fractions was utilized in the present work to describe the multiphase flow behaviour in the computational domain [32]. To calculate the volume fraction of the dispersed and the continuous phases in each computational cell, a separate volume fraction equation was solved. The conservation equations of mass and momentum for the continuous (air) and dispersed (droplets) phases are discussed in this section.

The mass conservation equation in the Eulerian approach is used in the present model as follows [32]:

$$\frac{\partial(\alpha_i \rho_i)}{\partial t} + \nabla \cdot \alpha_i \rho_i \vec{u}_i = 0, i = 1 \dots \dots N \tag{1}$$

where  $\alpha_i$ ,  $\rho_i$  and  $u_i$  are respectively, the volume fraction, density, and instantaneous velocity of phase  $i$ . The compatibility condition must be observed:  $\sum_{i=1}^N \alpha_i = 1$ . The momentum conservation equation used in the present model are given by [32]:

$$\frac{\partial(\alpha_i \rho_i u_i)}{\partial t} + \nabla \cdot (\alpha_i \rho_i u_i u_i) = -\alpha_i \nabla p + \nabla \cdot \alpha_i (\tau_i + T_i^t) + \alpha_i \rho_i f + M_{ij}, i = 1, \dots, N \tag{2}$$

where  $f$ ,  $p$ , and  $M_{ij}$  are respectively, the body force vector which includes the effect of gravity  $g$ , pressure which is assumed to be identical for all phases, and the momentum interfacial exchange between phases  $i$  and  $j$ . The phase  $i$

shear stress,  $\tau_i$ ,  $\tau_i = \mu_i \left[ (\nabla u_i + \nabla u_i^T) - \frac{2}{3} \nabla \cdot u_i \right]$ . In the current model, Reynolds stress,  $T_i^t$ , is simulated as follows [32]:

$$T_i^t = \mu_i^t \left[ (\nabla u_i + \nabla u_i^T) - \frac{2}{3} \nabla \cdot u_i I \right] - \frac{2}{3} \rho_i k_i I \tag{3}$$

Turbulent viscosity,  $\mu_i^t$ , is calculated using the following equation [32]:

$$\mu_i^t = C_\mu \rho_i \frac{K_i^2}{\epsilon_i} \tag{4}$$

where  $K_i$  and  $\epsilon_i$  are respectively, the turbulent kinetic energy and dissipation rate of energy. For the turbulent flow regime, the standard  $k$ - $\epsilon$  model [35] is used. In this model, the turbulent kinetic energy  $k$  and the dissipation rate  $\epsilon$  given by the following form [32]:

The turbulent kinetic energy:

$$\frac{\partial(\rho k)}{\partial t} + \frac{\partial(\rho U_j k)}{\partial X_j} = -\rho u_j \bar{u}_j \frac{\partial U_j}{\partial X_j} + \frac{\partial}{\partial X_j} \left( \mu + \frac{\mu_t}{\sigma_k} \frac{\partial k}{\partial X_j} \right) - \rho \epsilon \tag{5}$$

Dissipation rate of energy:

$$\frac{\partial(\rho \epsilon)}{\partial t} + \frac{\partial(\rho U_j \epsilon)}{\partial X_j} = -C_{\epsilon 1} \rho u_j \bar{u}_j \frac{\partial U_j}{\partial X_j} \frac{\epsilon}{k} + \frac{\partial}{\partial X_j} \left( \mu + \frac{\mu_t}{\sigma_\epsilon} \frac{\partial \epsilon}{\partial X_j} \right) - C_{\epsilon 2} \rho \frac{\epsilon^2}{k} \tag{6}$$

The momentum exchange between phases due to drag force and turbulent dispersion force is significant. The momentum interfacial exchange between air and droplets phases are taken into account. The momentum interfacial exchange by considering the drag force is given as [32]:

$$M_p = C_D \frac{1}{8} \rho_p A_i''' |V_r| V_r = -M_q \tag{7}$$

where  $C_D$ ,  $\rho_p$ ,  $A_i'''$ , and  $V_r$ , are respectively, the drag coefficient, density of primary phase (p), the interfacial area density, and the drift velocity. The drag coefficient  $C_D$  is given as a function of Reynolds number [36]:

$$C_D = \frac{4}{3} g d_p \frac{[\rho_p - \rho_g]}{\rho_g V_o^2} \tag{8}$$

where  $\rho_p$  and  $\rho_g$  are respectively density of droplets and air,  $d_p$  is the diameter of the droplet and  $V_o$  is the terminal velocity. The gravity that causes in the sedimentation of particles is considered to be one of important physical mechanism to eliminate droplets from room air. This mechanism depends on the droplets size and its terminal velocity. As mentioned earlier, the size of the droplet used in the present investigation was 1  $\mu\text{m}$  and their terminal velocity was calculated at room temperature (i.e. 20 °C) [4, 37].

## Initial and boundary conditions

The boundary conditions are an important factor influencing the accuracy of the flow computation and how accurately it represents the physical situation. The manner in which the boundary conditions are imposed also influences the convergence properties of the solution. In this work wall boundary, inlet and outlet boundaries are applied. Air mass flow rate at the mouth surface of each individual was described by sine function which fit quite well with normal human breathing process [7]. At the outlet, a pressure boundary condition with atmospheric pressure has been used. In the present model, no-slip wall boundary conditions are set at the walls for both phases (i.e. air & droplets). Initial conditions have to be specified for the dependent variables to achieve a unique solution of the governing equations. Everywhere in the computational domain, a volume fraction of the gas phase (i.e. air) is set to unity and the droplets volume fraction is set to zero. In the present study, droplet evaporation was neglected. This is a deficiency of the present model, as droplet evaporation plays a singularly important role in the eventual fate of a droplet. The droplet evaporation rate increases with higher temperature and lower relative humidities [5], which is not the case in the present model.

## Results and discussions

Although, there is no available data on how many SARS-CoV-2 particles come out with every breath of an infected individual. The ability to predict the number of inhaled aerosol droplets will give us an indication on the probability of contracting COVID-19. Not all aerosols droplets would carry viruses but part of them could. The present CFD model predicts the number of aerosol droplets inhaled by other individuals inside enclosed space through breathing and speaking only. The simulations were carried out in an enclosed space with dimensions of 4.5 m-width  $\times$  6 m-length  $\times$  3 m-height which was occupied with four individuals, one of them was assumed to be infected with COVID-19. The distance between the individuals is assumed to be 1.5 m. Two cases were investigated; case-1, the room was naturally ventilated with air coming in through the door. While, in case-2, the door was closed, and the room was ventilated with a constant airflow of  $0.045 \text{ m}^3 \cdot \text{sec}^{-1}$  through two holes were located on the ceiling of the room. While the gap under the door was used as an outlet. Figures 2 and 3 present the predicted results obtained from case-1 (i.e. room was naturally ventilated with air coming in through the door). The number of inhaled aerosol droplets by healthy individuals through breathing only is shown in Fig. 2. It can be seen from the data in Fig. 2 that, although the distance between the individuals was kept 1.5 m, person-C inhaled

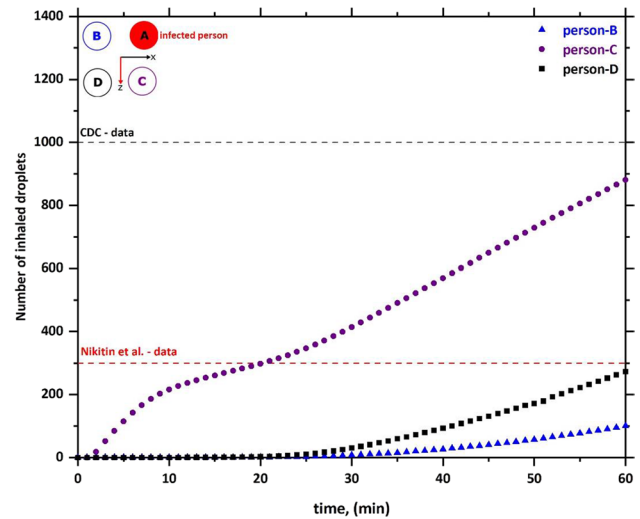


**Fig. 2** Number of inhaled droplets/particles by healthy individuals in an enclosed space – through breathing only

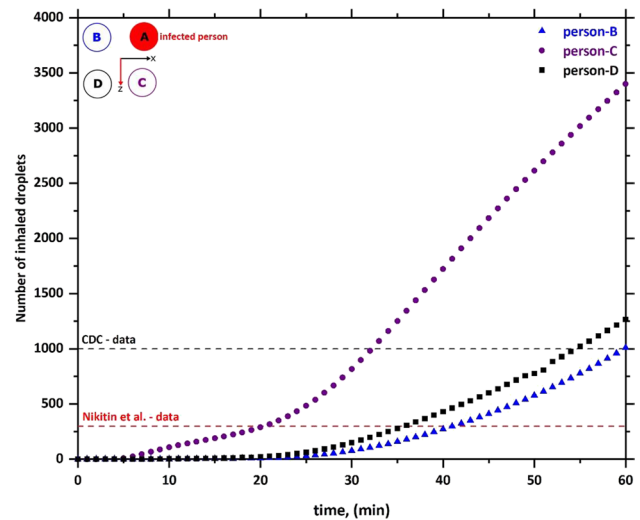
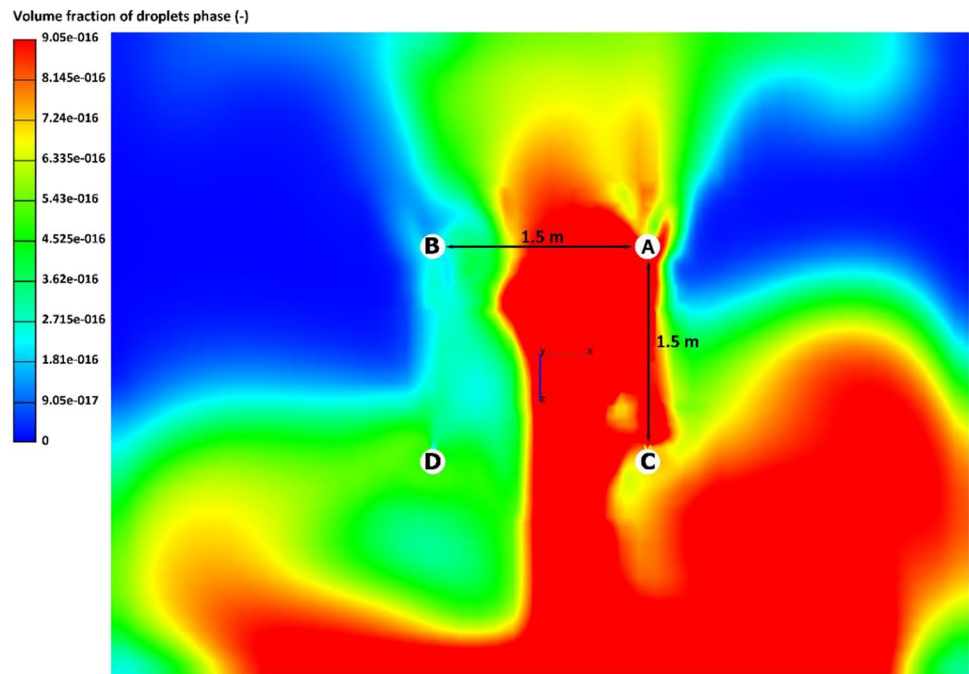


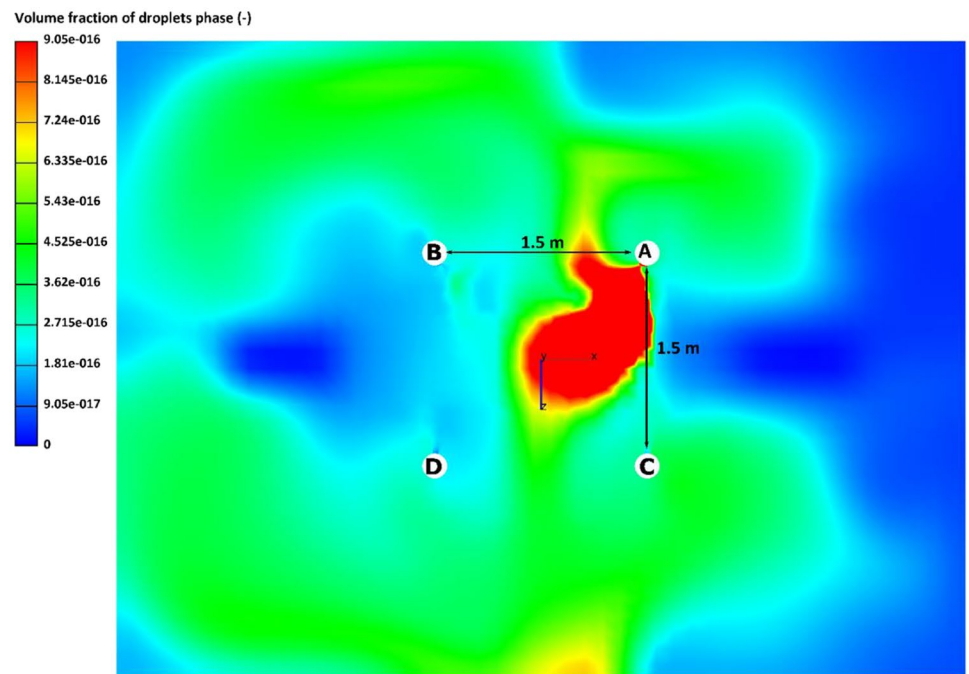
**Fig. 3** Number of inhaled droplets/particles by healthy individuals in an enclosed space – through speaking

more than 300 aerosol droplets after only 20 min and more than 800 droplets after 50 min. These results suggest that the social distancing (i.e. 1.5 m) is not adequate to reduce the risk of contracting diseases like COVID-19, especially when staying for a longer period in a closed space. Figure 2 also shows that the other two persons (i.e. person-B & person-D) will inhale less than 300 droplets in 60 min. The number of inhaled droplets by person-D was greater than the number of inhaled droplets by person-B. These results indicated that the location of the person with respect to the infected individual has a great effect on the number of inhaled droplets. As the two persons facing the infected person inhaled droplets more than the person standing next

**Fig. 4** Contour plots of volume fraction of droplets phase from speaking located at vertical height of 1.534 m. **(a)** case-1, the room was naturally ventilated with air incoming through the door. **(b)** case-2, the room was ventilated with constant air flow of  $0.045 \text{ m}^3 \cdot \text{sec}^{-1}$



(a). case-1, the room was naturally ventilated with air incoming through the door

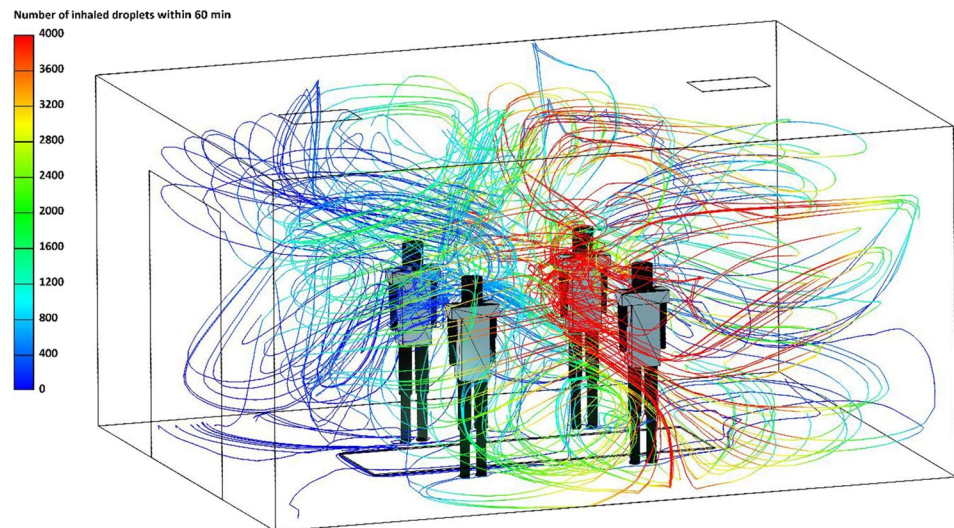


(b). case-2, the room was ventilated with a constant airflow of  $0.045 \text{ m}^3 \cdot \text{sec}^{-1}$

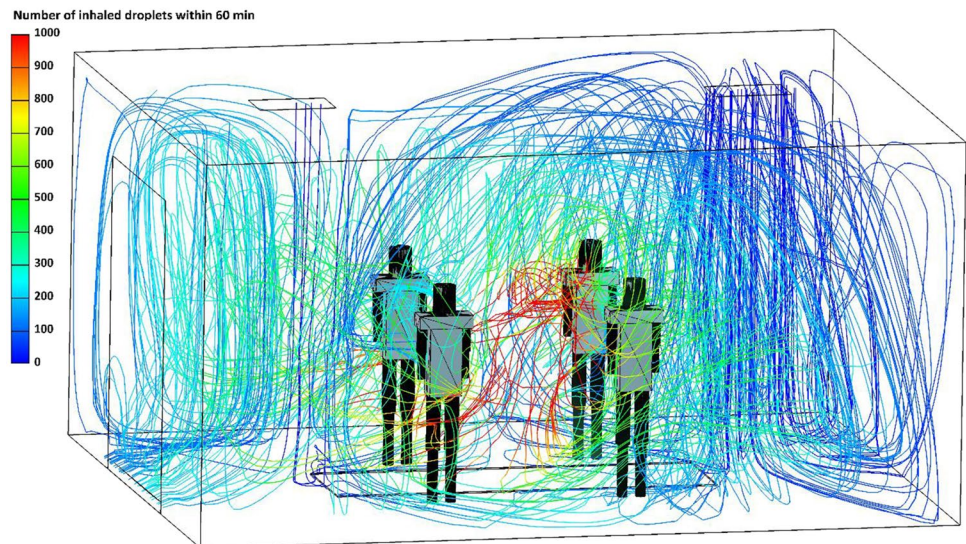
to him. On the other hands, the number of inhaled droplets by the healthy individuals dramatically increased in the case where an infected person is speaking (i.e. see Fig. 3). Figure 3 shows that person-C inhaled more than 1000 aerosol droplets within 30 min. While person-D inhaled more than 1000 droplets within 55 min.

The present study considered air and droplets as two different independent phases. The use of this assumption enables us to track the volume fraction of the droplet phase throughout the computational domain and thus predict the number of droplets in the computational domain. The volume fraction of droplets phase for the infected person

**Fig. 5** Visualizations demonstrating the effect of room ventilation type on the modelled spreading of the speak-released aerosol cloud. **(a)** case-1, the room was naturally ventilated with air incoming through the door. **(b)** case-2, the room was ventilated with constant air flow of  $0.045 \text{ m}^3 \cdot \text{sec}^{-1}$



(a). case-1, the room was naturally ventilated with air incoming through the door.

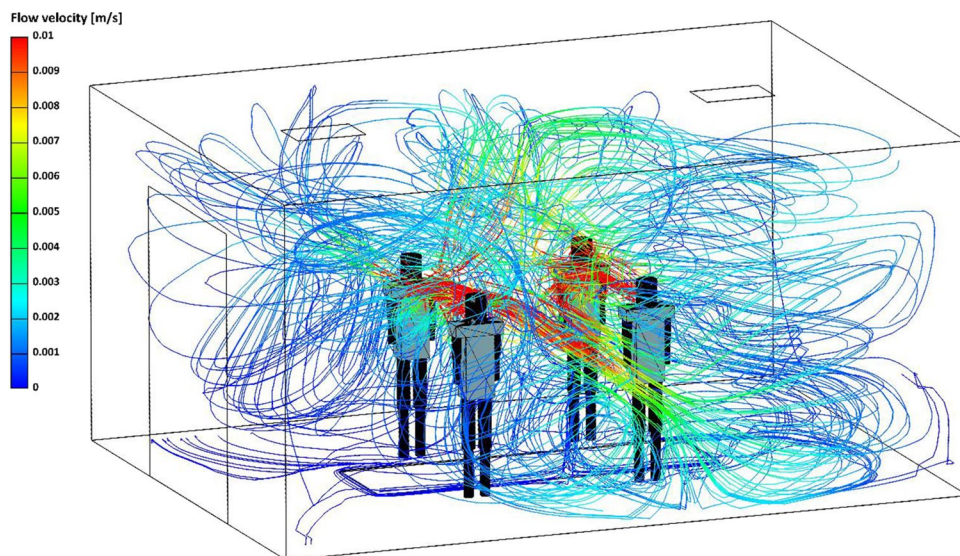


(b). case-2, the room was ventilated with constant air flow of  $0.045 \text{ m}^3 \cdot \text{sec}^{-1}$

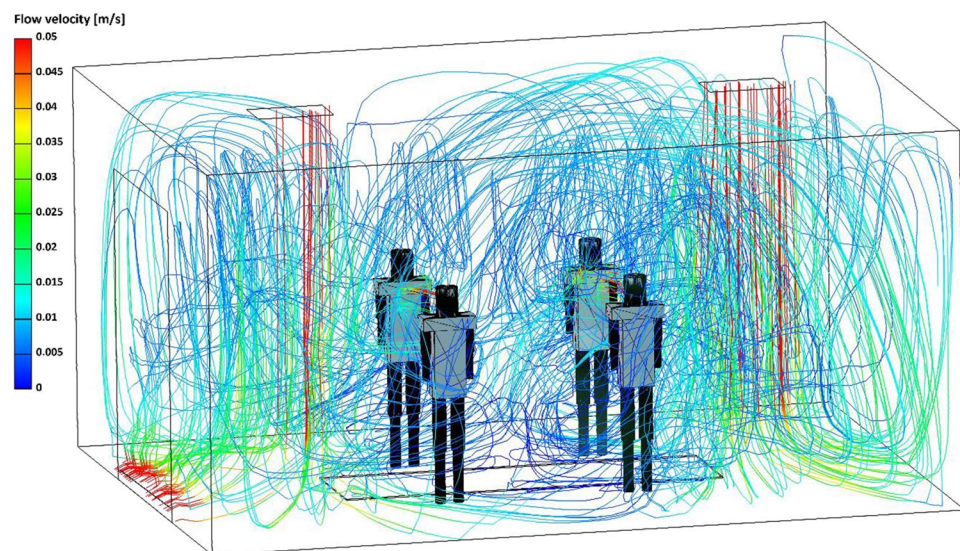
speaking case is presented in Fig. 4. The colour scale at the left of the figures illustrates the change in a volume fraction and also the number of droplets per cubic meter. The predicted results of this work are found to be in line with previous studies [7, 27]. The obtained results suggest that the ventilation has a great effect on the distribution of droplets phase. It can be seen from Fig. 4(a and b) that the volume fraction of droplets phase was significantly decreased in the computational domain when the ventilation was included in the CFD model. For example, at a distance of 1 m from the infected person, approximately 60% reduction in the droplet volume fraction was observed when ventilation was included in the model.

Figure 5(a and b) illustrates the number of inhaled droplets per person in 60 min from an infected person speaking. The obtained results suggest that the number of droplets inhaled per person can be significantly reduced with efficient ventilation design. Approximately more than 65% decrease in the number of inhaled droplets was observed when the room is well ventilated. For example, in case-1, person-C inhaled more than 1000 aerosol droplets in 30 min. While the same person was found to inhale only 360 droplets in 60 min in case-2. To explain these results, it is essential to understand the types of forces acting on the aerosol droplets. As mentioned earlier, the gravity force is responsible for the downward movement of the aerosol droplets. While

**Fig. 6** The airflow streamlines velocities at  $t=60$  min for ventilation during the room simulation. **(a)** case-1, the room was naturally ventilated with air incoming through the door. **(b)** case-2, the room was ventilated with constant air flow of  $0.045 \text{ m}^3 \cdot \text{sec}^{-1}$



(a). case-1, the room was naturally ventilated with air incoming through the door.



(b). case-2, the room was ventilated with constant air flow of  $0.045 \text{ m}^3 \cdot \text{sec}^{-1}$ .

the drag force which opposes the gravity, force is responsible for keeping aerosol droplets suspended in the air. The smaller size of the aerosol droplets, the less its mass and therefore the lower its rate at which it settles. Air currents coming from the ventilation holes represents extra drag force which will act in the same direction of gravity force. This extra force forces most of the droplets to settle down on the ground. This explains the significant decrease in the number of inhaled droplets by healthy individuals in the case-2 (i.e. with ventilation). Although in case-2, the only person directly facing the infected person will inhale more than 360 droplets in 60 min, we have to keep in mind that these results were obtained for speaking only with a limited number of

people in the room. The situation would be much worse if the population density would be higher or the number of droplets from coughing and sneezing was included in the model. It is well known that the size of droplets that are produced from coughing or sneezing is much larger than from the size of droplets produced through speaking or breathing which means they will settle quickly [1, 10, 13, 27, 38]. But these droplets from coughing or sneezing could travel for long distances and with high speeds which may reach more than 8 m [1, 10]. Therefore 1.5 m distance will not be enough to protect the healthy individuals from the droplets coming from an infected person. Also, the situation may become worse with the change of the air ventilation system.



For example, if the ventilation air supply is from the wall instead of a ceiling, the situation may become worse.

The transport equations for all phases throughout the whole domain are solved to cater for the transient dynamic situation in the domain and to account for variations of the flow with time caused by cyclic breathing. Flow velocity streamlines of case-1 and case-2 are shown in Fig. 6a and b. Figure 6a and b clearly show that the airflow inside the room was completely dominated by cyclic breathing in case-1, while in case-2, the flow circulation in the room is dominated by the ventilation air. The ventilation air creates a state air circulation inside the room, which has a significant effect on the aerodynamics of droplets and their settling velocities. These observations support what was explained in the previous paragraph on the effect of ventilation type on the concentration of inhaled droplets by healthy individuals.

## Summary and conclusions

In this study, Computational Fluid Dynamics (CFD) was utilized to examine the feasibility of social distancing (i.e. 1.5 m) in closed spaces taking into account the possibility for airborne transmission of SARS-CoV-2. The developed CFD model was used to simulate human respiration activities, such as breathing and speaking within indoor environments. The main findings of the present work can be summarised as follows:

- Although the distance between the individuals was kept 1.5 m. The person directly facing the infected person inhaled more than 300 aerosol droplets after only 20 min and more than 800 droplets after 50 min.
- Location of the person with respect to the infected individual has a great effect on the number of inhaled droplets.
- The number of droplets was significantly decreased in room when the ventilation was included in the CFD model.
- Approximately 65 % decrease in the number of inhaled droplets was observed when the room is well ventilated.

**Acknowledgements** Authors would like to acknowledge the Centre for Astrophysics and Supercomputing for offering the supercomputing resources for the present work. The authors wish to thank Mr. Warren Hack (Senior Client Support Analyst-Swinburne University of Technology) for his technical support.

**Data availability** The data that support the findings of this study are available on request from the authors.

## Declarations

**Consent for publication** Not applicable.

**Ethics approval and consent to participate** Not applicable.

**Conflict of interest** The authors declare that they have no conflict of interest.

## References

1. World Health Organization (WHO). Coronavirus disease (COVID-19) pandemic, 2021, May 25. <https://www.who.int/emergencies/diseases/novel-coronavirus-2019>.
2. Australia Government Department of Health. What you need to know about coronavirus (COVID-19), Department of Health, 2021, April 6. <https://www.health.gov.au/news/health-alerts/novel-coronavirus-2019-ncov-health-alert/what-you-need-to-knowabout-coronavirus-covid-19>.
3. Lu J, Gu J, Li K, Xu C, Su W, Lai Z, Zhou D, Yu C, Xu B, Yang Z. *Emerg Infect Dis.* 2020;26(7):1628–31. <https://doi.org/10.3201/eid2607.200764>.
4. Scheuch G. *J Aerosol Med Pulm Drug Deliv.* 2020;33(4):230–4. <https://doi.org/10.1089/jamp.2020.1616>.
5. Mittal R, Ni R, Seo J-H. *J Fluid Mech.* 2020;894:F2. <https://doi.org/10.1017/jfm.2020.330>.
6. Hui DS, Chow BK, Lo T, Tsang OTY, Ko FW, Ng SS, Gin T, Chan MTV. *Eur Respir J.* 2019;53(4):1802339. <https://doi.org/10.1183/13993003.02339-2018>.
7. Leonard S, Strasser W, Whittle JS, Volakis LI, DeBellis RJ, Prichard R, Atwood CW Jr, Dungan GC II. *J Am Coll Emerg Physicians Open.* 2020;1(4):578–91. <https://doi.org/10.1002/emp2.12158>.
8. Riediker M, Tsai DH. *JAMA Netw Open.* 2020;3(7):e2013807. <https://doi.org/10.1001/jamanetworkopen.2020.13807>.
9. van Doremalen N, Bushmaker T, Morris DH, Holbrook MG, Gamble A, Williamson BN, Tamin A, Harcourt JL, Thornburg NJ, Gerber SI, Lloyd-Smith JO, de Wit E, Munster VJ. *N Engl J Med.* 2020;382(16):1564–7. <https://doi.org/10.1056/NEJMc2004973>.
10. Centers for Disease Control and Prevention (CDC). About COVID-19, 2021, March 21. <https://www.cdc.gov/>.
11. Anderson EL, Turnham P, Griffin JR, Clarke CC. *Risk Anal.* 2020;40(5):902–7. <https://doi.org/10.1111/risa.13500>.
12. Asadi S, Bouvier N, Wexler AS, Ristenpart WD. *Aerosol Sci Technol.* 2020;0(0):1–4. <https://doi.org/10.1080/02786826.2020.1749229>.
13. Morawska L, Cao J. *Environ Int.* 2020;139:105730. <https://doi.org/10.1016/j.envint.2020.105730>.
14. Liu Y, Ning Z, Chen Y, Guo M, Liu Y, Gali NK, Sun L, Duan Y, Cai J, Westerdahl D, Liu X, Xu K, Ho KF, Kan H, Fu Q, Lan K. *Nature.* 2020;582(7813):557–60. <https://doi.org/10.1038/s41586-020-2271-3>.
15. Duguid JP. *J Hyg (Lond).* 1946;44(6):471–9. <https://doi.org/10.1017/s0022172400019288>.
16. Fairchild C, Stampfer J. *Am Ind Hyg Assoc J.* 1987;48(11):948–9.
17. Papineni RS, Rosenthal FS. *J Aerosol Med.* 1997;10(2):105–16. <https://doi.org/10.1089/jam.1997.10.105>.
18. Edwards DA, Man JC, Brand P, Katstra JP, Sommerer K, Stone HA, Nardell E, Scheuch G. *Proc Natl Acad Sci U S A.* 2004;101(50):17383–8. <https://doi.org/10.1073/pnas.0408159101>.

19. Fabian P, McDevitt JJ, DeHaan WH, Fung RO, Cowling BJ, Chan KH, Leung GM, Milton DK. PLoS One. 2008;3(7):e2691. <https://doi.org/10.1371/journal.pone.0002691>.
20. Chao CYH, Wan MP, Morawska L, Johnson GR, Ristovski Z, Hargreaves M, Mengersen K, Corbett S, Li Y, Xie X. J Aerosol Sci. 2009;40(2):122–33.
21. Morawska L, Johnson G, Ristovski Z, Hargreaves M, Mengersen K, Corbett S, Chao CYH, Li Y, Katoshevski D. J Aerosol Sci. 2009;40(3):256–69.
22. Han ZY, Weng WG, Huang QY. J R Soc Interface. 2013;10(88):20130560. <https://doi.org/10.1098/rsif.2013.0560>.
23. Xie X, Li Y, Sun H, Liu L. J R Soc Interface. 2009;6(Suppl\_6):S703–14. <https://doi.org/10.1098/rsif.2009.0388.focus>.
24. Asadi S, Wexler AS, Cappa CD, Barreda S, Bouvier NM, Ristenpart WD. Sci Rep. 2019;9(1):2348. <https://doi.org/10.1038/s41598-019-38808-z>.
25. Ciric L. One metre or two? The science behind social distancing, The Conversation, 2020, June 18. <https://theconversation.com/one-metre-or-two-the-science-behind-social-distancing-139929>.
26. Blocken B, Malizia F, Van Druenen T, Marchal T. 2020. Towards aerodynamically equivalent COVID19 1.5 m social distancing for walking and running. Preprint. [https://www.euroga.org/system/1/user\\_files/files/000/045/111/45111/150d3060c/original/Social\\_Distancing\\_v20\\_White\\_Paper.pdf](https://www.euroga.org/system/1/user_files/files/000/045/111/45111/150d3060c/original/Social_Distancing_v20_White_Paper.pdf).
27. Vuorinen V, Aarnio M, Alava M, Alopaeus V, Atanasova N, Auvinen M, Balasubramanian N, Bordbar H, Erasto P, Grande R, Hayward N, Hellsten A, Hostikka S, Hokkanen J, Kaario O, Karvinen A, Kivisto I, Korhonen M, Kosonen R, Kuusela J, Lestinen S, Laurila E, Nieminen HJ, Peltonen P, Pokki J, Puisto A, Raback P, Salmenjoki H, Sironen T, Osterberg M. Saf Sci. 2020;130:104866. <https://doi.org/10.1016/j.ssci.2020.104866>.
28. Nikitin N, Petrova E, Trifonova E, Karpova O. Influenza virus aerosols in the air and their infectiousness. Advances in virology. 2014. <https://doi.org/10.1155/2014/859090>
29. Ai ZT, Melikov AK. Indoor Air. 2018;28(4):500–24. <https://doi.org/10.1111/ina.12465>.
30. Yan J, Grantham M, Pantelic J, Bueno de Mesquita PJ, Albert B, Liu F, Ehrman S, Milton DK, Consortium E. Proc Natl Acad Sci U S A. 2018;115(5):1081–6. <https://doi.org/10.1073/pnas.1716561115>.
31. Yip L, Finn M, Granados A, Prost K, McGeer A, Gubbay JB, Scott J, Mubareka S. J Occup Environ Hyg. 2019;16(5):341–8. <https://doi.org/10.1080/15459624.2019.1591626>.
32. AVL FIRE. Software Documentation, 2020 R1 ed. Austria: Graz; 2021.
33. Sarhan AR, Naser J, Brooks G. Sep Sci Technol. 2017;53(1):181–97. <https://doi.org/10.1080/01496395.2017.1375525>.
34. Patankar SV, Spalding DB. Numerical Prediction of Flow, Heat Transfer, Turbulence and Combustion. In Patankar SV, Pollard A, Singhal AK, Vanka SP, editors. Oxford: Pergamon: 1983. p. 54–73.
35. Launder BE, Spalding DB. Comput Methods Appl Mech Eng. 1974;3(2):269–89. [https://doi.org/10.1016/0045-7825\(74\)90029-2](https://doi.org/10.1016/0045-7825(74)90029-2).
36. Donald F, Elger BAL, Clayton T, Crowe JA, Roberson. Engineering Fluid Mechanics. Hoboken: Wiley Direct; 2019.
37. Concept Smoke Systems. Particle Size & Settling Velocities, 2020 June 17. <http://www.smokemachines.com/settlingvelocities-particle-size.aspx>.
38. Bhagat RK, Davies Wykes MS, Dalziel SB, Linden PF. J Fluid Mech. 2020;903:F1. <https://doi.org/10.1017/jfm.2020.720>.

**Publisher's note** Springer Nature remains neutral with regard to jurisdictional claims in published maps and institutional affiliations.